archives
of thermodynamics
Vol. **33**(2012), No. 2, 85–106
DOI: 10.2478/v10173-012-0012-1

Energy consumption in terms of shear stress for two types of membrane bioreactors used for municipal wastewater treatment processes

NICOLAS RATKOVICH*
THOMAS R. BENTZEN
MICHAEL R. RASMUSSEN

Department of Civil Engineering, Aalborg University, Sohngaardsholmsvej 57, DK-9000 Aalborg, Denmark

Abstract Two types of submerged membrane bioreactors (MBR): hollow fiber (HF) and hollow sheet (HS), have been studied and compared in terms of energy consumption and average shear stress over the membrane wall. The analysis of energy consumption was made using the correlation to determine the blower power and the blower power demand per unit of permeate volume. Results showed that for the system geometries considered, in terms the of the blower power, the HF MBR requires less power compared to HS MBR. However, in terms of blower power per unit of permeate volume, the HS MBR requires less energy. The analysis of shear stress over the membrane surface was made using computational fluid dynamics (CFD) modelling. Experimental measurements for the HF MBR were compared with the CFD model and an error less that 8% was obtained. For the HS MBR, experimental measurements of velocity profiles were made and an error of 11% was found. This work uses an empirical relationship to determine the shear stress based on the ratio of aeration blower power to tank volume. This relationship is used in bubble column reactors and it is extrapolate to determine shear stress on MBR systems. This relationship proved to be overestimated by 28% compared to experimental measurements and CFD results. Therefore, a corrective factor is included in the relationship in order to account for the membrane placed inside the bioreactor.

Keywords: Shear stress; Bubble column; CFD; Membrane bioreactor (MBR)

*Corresoponding author. E-mail address: nr@civil.aau.dk

Nomenclature

A	–	membrane area, m^2
A_x	–	open cross-sectional area, m^2
C_0	–	bulk concentration of ferricyanide, = 3 mol/m^3
D	–	diffusion coefficient of ferricyanide, $6.6 \times 10^{-10} m^2/s$
d	–	external doameter of the fiber for HF, m
d_e	–	diameter of the probe, m
e	–	blower efficiency, ∼0.56
E_A	–	blower power consumption, kW
F	–	Faraday constant, = 96500 C/mol
G	–	amplifier gain, = 1000
g	–	gravity acceleration, = 9.81 m^2/s)
h	–	height of water above the air diffuser, m
J	–	permeate flux, m/h
L	–	length of the membrane module, m
p_{atm}	–	atmospheric pressure, = 101 325 Pa
Q_A	–	air flow rate, m^3/h
Q_p	–	permeate flow, m^3/h
R	–	resistance, = 100 Ω
SAD_m	–	specific aeration demand imparted to the membrane, m/h
SAD_p	–	specific aeration demand imparted to the permeate volume
T	–	inlet temperature, K
U	–	module upflow aeration velocity, m/h
V	–	volume of fluid, m^3
V_0	–	voltage signal, V
W_m	–	blower power per unit membrane area, kW/m^2
W_p	–	blower power demand per unit of permeate volume, kWh/m^3

Greek symbols

δ	–	channel space separation for HS, m
φ	–	packing density for HF, m^2/m^3
$\dot{\gamma}$	–	shear rate, s^{-1}
λ	–	ratio of specific heat capacity at constant pressure to specific heat capacity at constant volume, = 1.4 for air
μ	–	viscosity, Pa s
ν_e	–	number of electrons involved in the reaction, = 1
ρ_w	–	density of water, 998.28 kg/m^3 at 20 °C
τ	–	shear stress, Pa

1 Introduction

Biological wastewater treatment processes (WWTP) consist of two main steps. The first step is the biological removal of organic substances and nutrients followed by solids-water separation. The latter step is either achieved through gravity, known as conventional activated sludge (CAS) (Fig. 1) or

by membrane filtration, known as membrane bioreactors (MBR) (Fig. 2). The latter gives rise to superior effluent quality compared to the CAS.

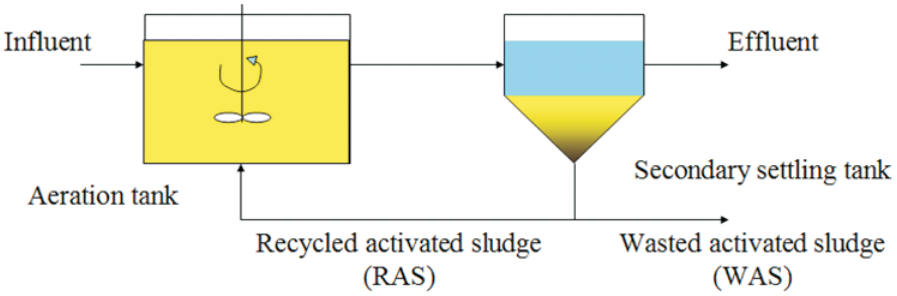

Figure 1. Conventional activated sludge systems.

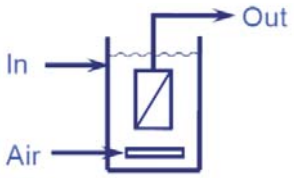

Figure 2. Submerged membrane bioreactors [1].

The MBR hydrodynamics are similar to bubble columns operation, with the difference that a membrane is placed inside the bubble column to extract the clean water. The placement of the membrane inside the column affects behaviour of the bubbles [2–4]. The main drawback of MBR systems is the fouling of the membrane, which results in frequent cleaning and replacement, making this system less appealing for full-scale applications [1]. This hampers its commercialization due to reduction of productivity and increased maintenance and operational cost.

This membrane fouling is caused by the attachment of suspended solids and soluble substances on the membrane surface. It is the major barrier for a widespread application of MBR technology. Different types of fouling can be identified [5,6]:

- Clogging is a progressive accumulation of dry sludge in module volume, starting from "dead zones" in the reactor.
- Sludging refers to an accumulation of sludge at the surface of the membrane.

- Fouling represents all mechanisms of cake building, plus adsorption/ blockage into membrane material.

In MBR, the hydrodynamics are of great importance for reducing sludge deposition on the membrane surface and prolonging the operating period below the critical trans membrane pressure (TMP). Membrane performance measured in terms of membrane fouling was observed to be enhanced by gas sparging, and reports have shown improvements up to 63% when air is introduced [7–9]. Several mechanisms were identified: 1) bubble-induced secondary flow, 2) physical displacement of the mass transfer boundary layer and 3) pressure pulsing caused by slugs [10]. It has been found that bubbling can limit surface fouling (clogging and sludging), but not internal fouling (adsorption and pore blockage).

A comprehensive review of the effects of aeration on submerged MBRs reported that coarse rather than fine bubbling is the preferred mode to control fouling [10]. A general observation is that larger airflow rates decrease the rate at which the pressure rises due to fouling, but that enhancement reaches a plateau as gas flow rate increases [11].

The benefits of bubbling appear to be most effective at low liquid velocities. At high liquid velocities, the performance becomes dominated by bulk liquid shear [10]. Studies on the gas sparging focus on the effect of overall gas flow rates, bubble size, and frequency [12,13]. When bubbling is applied to the filtration processes, it was found that the fluctuation in shear stress affected the flux more than the absolute value of shear stresses induced by the bubbles. The peak of shear stresses induced by bubbling were up to 45% higher compared to when no bubbling was applied [14,15]. It is important to highlight that the effect of shear stresses induced by gas sparging on fouling control is not well understood, as a result, a trial-and-error approach is required in order to find the best air sparging strategies. Nevertheless, the energy used for adding air into the system is a significant component of the operating cost for MBR systems (i.e. up to 40% of the total energy consumption). That is the main reason why a hydrodynamic model of submerged MBR is required to better understand the shear stress induced by air sparging, and to identify optimal air sparging scenarios and membrane module configurations that optimize the magnitude and distribution of shear stress. Therefore, dedicated experiments are needed to fully understand the hydrodynamics of this two-phase flow. Moreover, insight can be obtained using computational fluid dynamics (CFD). CFD hydrodynamic models are commonly used for design and optimization of

processes. This study gives an overview of recent development using CFD in modelling hydrodynamics in two types of submerged MBR systems: 1) hollow fiber (HF) (GE – Zenon) MBR, and 2) hollow sheet (HS) (Alfa Laval) MBR.

2 Materials and methods

2.1 Membrane aeration

Aeration is necessary in order to have a scouring effect over the membrane surface. In practice, the membrane aeration value is not defined theoretically since the relationship between aeration and permeate flux decline is currently not well understood [1,16]. The contributing factor to energy demand in submerged systems is the specific aeration demand imparted to the membrane (SAD_m), which is the ratio of aeration rate (Q_A in m^3/h) to membrane area (A in m^2) as

$$SAD_m = \frac{Q_A}{A} \, . \tag{1}$$

The specific aeration demand imparted to the permeate volume attained (SAD_p) is the ratio of aeration rate to permeate flow (Q_p in m^3/h) following equation:

$$SAD_p = \frac{Q_A}{Q_p} \, . \tag{2}$$

The aeration rate (Q_A) and the permeate flow (Q_p) are defined respectively

$$Q_A = UA_x \, , \tag{3}$$

$$Q_p = JA \, , \tag{4}$$

where J is the permeate flux (m/h), A_x is the open cross-sectional area (m^2) and U is the module upflow aeration velocity. The air flow velocity in the channels for the hollow fiber (HF) and hollow sheet (HS) are defined as follows [17].

$$U = \frac{2L\,SAD_m}{\delta} \, , \tag{5}$$

$$U = \frac{L\,SAD_m}{(\frac{1}{\varphi} - \frac{d}{4})} \, , \tag{6}$$

where L is the length of the membrane module in m, δ is the channel space separation in m for the HS, φ and d are the packing density [m^2/m^3], and external diameter of the fiber [m], respectively, for the HF.

For a given aerator system at a fixed depth in the tank, the blower power consumption (E_A in kW) is defined by [1,18]:

$$E_A = kQ_A \ , \tag{7}$$

where

$$k = \frac{p_{atm} T \lambda}{2.73 \times 10^5 e(\lambda - 1)} \left[\left(\frac{p_{atm} + \rho_w g h}{p_{atm}} \right)^{1 - \frac{1}{\lambda}} - 1 \right] \tag{8}$$

and p_{atm} is the atmospheric pressure (= 101 325 Pa), T is the inlet temperature [K], e is the blower efficiency (~ 0.56), λ is the ratio of specific heat capacity at constant pressure to specific heat capacity at constant volume ($c_p/c_v = 1.4$ for air), ρ_w is the density of water (998.28 kg/m^3 at 20 °C), g is the gravity acceleration (= 9.81 m^2/s) and h is the height of water above the air diffuser [m].

Dividing Eq. (7) by the total membrane module area (A) to which the flow rate (Q_A) applies, the power per unit membrane area (W_m in kW/m^2) is then obtained [1]

$$W_m = \frac{E_A}{A} = \frac{kQ_A}{A} \ . \tag{9}$$

which divided by the permeate flux (J) gives an expression for the membrane aeration blower power demand per unit of permeate volume (W_p in kWh/m^3) [1]

$$W_p = \frac{E_A}{JA} = \frac{kQ_A}{JA} = \frac{kUA_x}{JA} \ , \tag{10}$$

where A_x is the open cross-sectional area. Equation (10) shows two aspects regarding the design energy consumption for submerged MBR [17]: 1) the energy demand increases proportionally with A_x, which is higher for HS compared to HF. The limiting, lower value of A_x is related to the propensity of membrane channels to clog, and 2) the membrane area (A) can be increased by increasing the length of the module (L) without detriment to the required volumetric aeration rate (Q_A). However, increasing module length increases the aerator depth (h), which will increase the energy consumption.

2.2 Activated sludge viscosity

Viscosity (μ) is a property that influences the hydraulic regime and transport phenomena. It is defined as the ratio between shear stress (τ) and shear rate ($\dot{\gamma}$)

$$\mu = \frac{\tau}{\dot{\gamma}} \, . \tag{11}$$

The viscosity of Newtonian liquids (e.g. water) exhibits a linear shear stress and shear rate relationship and hence, a constant viscosity. However, some particulate suspensions (e.g. activated sludge in MBR), exhibit pseudoplastic (non-Newtonian) behaviour [19–22] where the apparent viscosity (μ_a) can be related to the shear rate according to a power-law relationship:

$$\mu_a = k\dot{\gamma}^{n-1} \, , \tag{12}$$

where k and n are the consistency index [Pas^n] and the flow behaviour index [–], respectively. For activated sludge in MBR, Rosenberger *et al.* [22] proposed empirical models for k and n as function of the total suspended solids (TSS) (g/L):

$$k = 0.001 \exp(2\, TSS^{0.41}) \, , \tag{13}$$

$$n = 1 - 0.23\, TSS^{0.37} \, . \tag{14}$$

2.3 Shear stress in bubble columns

In bubble columns, the power input per unit volume of liquid is related to the specific energy dissipation rate, which depends on the shear rate and shear [23]

$$\frac{E_A}{V} = \tau\dot{\gamma} \, , \tag{15}$$

where V in the volume of fluid (i.e. water volume above the air diffusers). Combining Eqs. (15) with (11) and Eqs. (15) with (12) for Newtonian and non-Newtonian fluids, respectively gives [23]

$$\tau = \left(\mu \frac{E_A}{V}\right)^{0.5} \, , \tag{16}$$

$$\tau = \left[k \left(\frac{E_A}{V}\right)^n\right]^{\frac{1}{n+1}} \, . \tag{17}$$

2.4 Experimental setup

2.4.1 Operational conditions

The operational condition of these two MBR systems is summarized in Tab. 1 and in Appx. A.

Table 1. Operational conditions of the two MBR systems.

Parameter	Unit	Symbol	HF	HS
Tank dimensions	m	H, W, L'	2.18, 0.85, 0.47	2.4, 1.78, 0.47
Tank volume	m^3	V_T	0.84	7.35
Water level above the air diffusers	m	h	2.03	1.96
Length of the membrane module	m	L	1.67	0.96
Water volume above the air diffusers	m^3	V	0.29	1.19
Air flow rate	m^3/h	Q_A	5, 10, 15	37, 55, 74
Membrane area	m^2	A	24.3	154
Packing density	m^2/m^3	φ	300	–
HF outside diameter	m	d	0.0019	–
HS channel separation	m	δ	–	0.007
Permeate flux	m^3/m^2h	J	0.03	0.03

2.4.2 HF MBR

The shear stresses were measured exclusively for the HF MBR system using an electrochemical method [24–26]. With this method, the shear stresses at a surface can be estimated based on the diffusion limited current passing from a cathode (shear probe), embedded flush to the outer surface of teflon tubes (similar in diameter and flexibility to the HF), to an anode, through a reversible ion couple solution in which the surface is submerged (electrolyte). A total of 60 shear probes were constructed. The shear intensity measured in volts can be converted to shear stress (in Pa) using

$$\tau = \mu \left(\frac{4.64\, V_0}{v_e F \pi_e^{5/3} C_0 D^{2/3} R G} \right)^3 = 9.755\, V_0^3 \,. \tag{18}$$

where V_0 is the voltage signal (V), R is the resistance (= 100 Ω), G is the amplifier gain (= 1000), v_e is the number of electrons involved in the reaction (= 1), F is the Faraday constant (= 96 500 C/mol), d_e is the

diameter of the probe (in m), C_o is the bulk concentration of ferricyanide (= 3 mol/m^3) and D is the diffusion coefficient of ferricyanide (6.6×10^{-10} m^2/s) at 16.5 °C [27].

The 36 shear probes (Fig. 3a) are located in the membrane modules for three coronal planes (Fig. 3b) [28]. The probes record the absolute wall shear stress value (no direction).

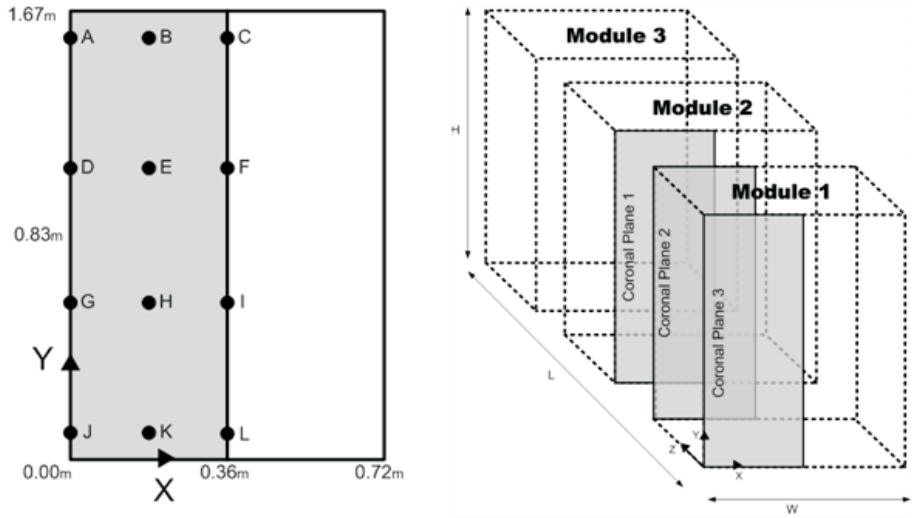

a) b)

Figure 3. Tested membrane modules: a) Shaded vertical sheets within three modules and area of interest, and b) location where shear forces were measured on each coronal plane [28].

2.4.3 HS MBR

Experimental shear stress measurements were not made for this system. Nevertheless, velocity measurements were performed using micropropellers (MP) inside the module channels and the results are presented in [29]. It is important to highlight that the experiments were carried out with air and water. Nevertheless, using water instead of activated sludge can give an insight into the hydrodynamics of the process.

2.5 Computational fluid dynamics models

Two CFD models were developed to simulate the two pilot-scale submerged MBR systems. The CFD packages used to simulate the HS module and the HF module were ANSYS CFX v13 [29] and ANSYS Fluent v6.3 [32], respectively, for which shear maps have been developed for different sparging conditions over the membrane surface (see Tab. 1). These CFD models contain the mixture model (also known as the algebraic slip mixture model (ASM)) which is a simplified multiphase model that allows the phases to move at different velocities. It assumes the phases to be in interpenetrating continua (nonmiscible). It models two phases by solving the momentum and the continuity equation for the mixture, the volume fraction equation for the secondary phase, and an algebraic expression for the relative velocity. It does not assume that there is an interface between the two immiscible phases and mass transfer is not allowed. This model is commonly used to modelling bubble columns. To properly capture the shear value at the wall of the membrane, a fine grid was built where the shear stress has an impact. The k-ε turbulence model with enhanced wall treatment was used to properly capture the shear stress at the membrane wall. This turbulence model is commonly used to modelling bubble columns [30]. To initialize the simulation, the system starts without gas (still liquid) and after the specific flow rate of the gas is defined for each diffuser, there is no inlet of liquid and no permeation occurring. To solve the momentum transport equation, the QUICK (quadratic upwind interpolation) scheme was used [31], which increases stability of the solution, provides a faster convergence and has 4th order accuracy. For pressure, the body force weighted (BFW) scheme was used which captures buoyancy and increases stability in the solution. For the pressure-velocity coupling, the pressure implicit solution by split operator method (PISO) scheme for faster convergence was used [31].

3 Results and discussion

3.1 Membrane aeration

The specific aeration demand for the membrane and for permeate volume , as well as aeration velocity, open x-sectional area, blower power, power per unit membrane area and per permeate flow are presented in Tab. 2. The blower power is shown in Fig. 4. As seen in Fig. 4, the HS MBR air blower consumes more energy compared to the HF MBR, which is expected as it

Table 2. Operating data based on Tab. 1 and Eqs. (1) to (10) for the two MBR systems.

	Q_A	SAD_m	U	SAD_p	A_x	E_a	W_m	W_p
Module	m^3/h	m/h	m/s	–	m^2	kW	kW/m^2	kWh/m^3
HS	37	0.24	0.02	8.01	0.561	0.367	0.0024	0.079
HS	55	0.36	0.03	11.90	0.561	0.546	0.0035	0.118
HS	74	0.48	0.04	16.02	0.561	0.734	0.0048	0.159
HF	5	0.21	0.03	6.86	0.042	0.048	0.0020	0.066
HF	10	0.41	0.07	13.72	0.042	0.096	0.0039	0.132
HF	15	0.62	0.10	20.58	0.042	0.144	0.0059	0.197

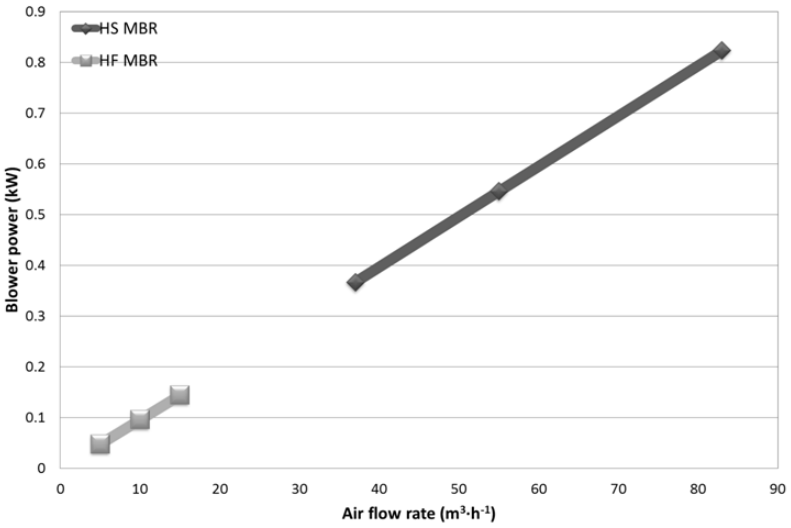

Figure 4. Blower power vs. air flow rate for the two MBR systems.

uses larger air flow rates. Based on that, the blower power per membrane area can be an indicator of the energy consumption, as it is shown in Fig. 5.

From Fig. 5 it is observed that using the blower power per membrane area, the HF MBR uses 20% less energy than the HS MBR at low air flow rate (5 m^3/h). However, once the air flow rate increases, the HS MBR requires 25% less energy that the HF MBR in terms of blower power. The final indicator in energy consumption, is related to the blower power per permeate flow and it is presented in Fig. 6. As seen in Fig. 6, using the blower power per permeate volume, the result is the same as when using

the blower power per membrane area. Therefore, as low air flow rates, the HF MBR is more efficient than the HS MBR. On the other hand, at larger flow rates, the HS MBR is more efficient than the HF MBR.

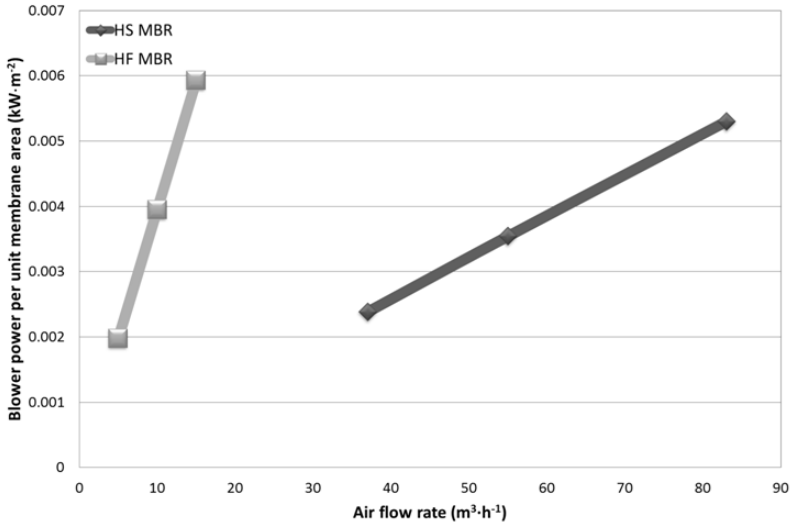

Figure 5. Blower power per unit of membrane area vs. air flow rate for the two MBR systems.

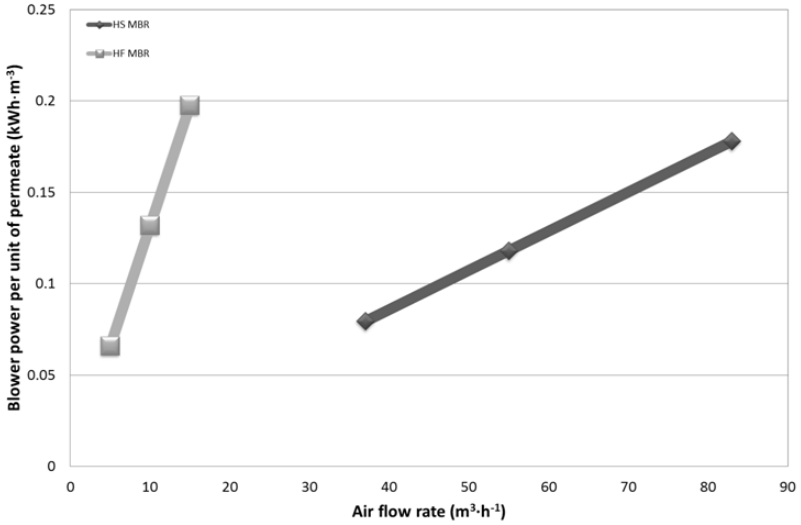

Figure 6. Blower power per unit of permeate volume vs. air flow rate for the two MBR systems.

3.2 CFD results

In the previous section, it was mentioned that the HS MBR performs better than the HF MBR in terms of energy consumption per membrane area and per permeate volume. However, it is necessary to determine the air distribution within the module and the shear stress over the membrane surface. For this reason a CFD model was built.

3.3 Air distribution

Figure 7 shows the distribution across the HF (Fig. 7a) and HS (Fig. 7b) MBR modules. The air is well distributed within the frame, and it is possible to see that there are no pronounced dead zones between the filtration sheets.

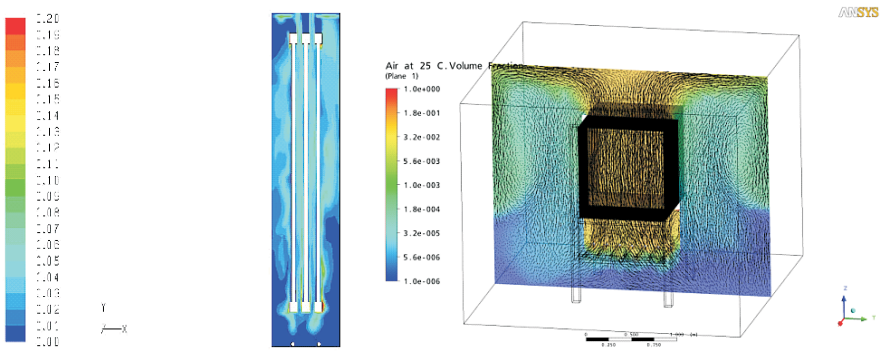

a) b)

Figure 7. Air volume fraction for: a) HF, and b) HS MBRs.

3.4 Wall shear stress

The particle scouring/shear stress (reduction of fouling) is generated from the cross flow induced by the air bubbles. A good agreement between the experimental measurements of shear stress and the CFD simulation was obtained (Fig. 8) [32]. The average shear stress estimated using CFD was similar in magnitude to the one measured experimentally. Nevertheless, the shear patter is not well represented by the CFD simulation. The reason for this is that the HFs are not completely fixed and they move and sway in the bundle due to the bubble induced turbulence. The overall average of shear

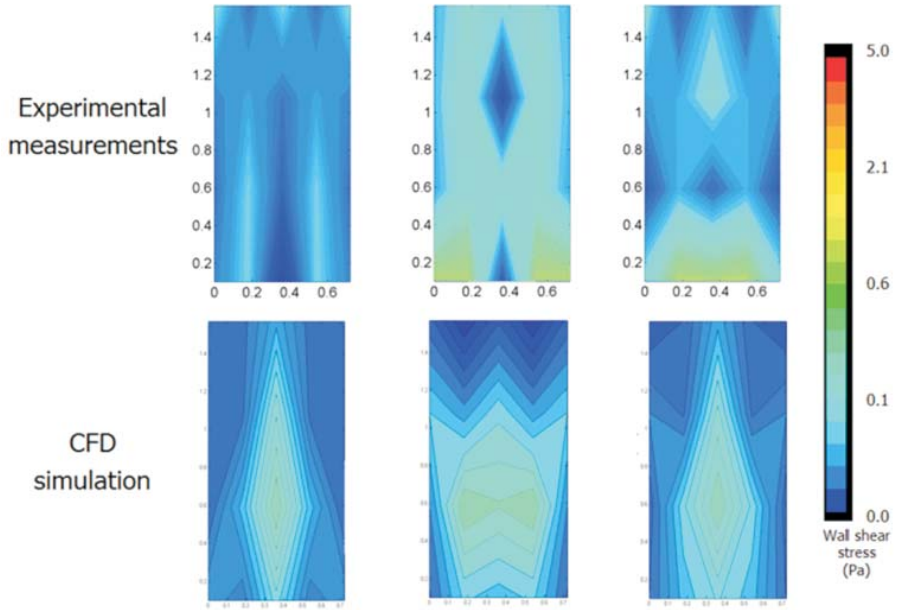

Figure 8. Comparison of the shear stress contours for the experimental measurements and CFD simulations for an air flow rate of 15 m^3/h for 3 different coronal planes (Fig. 3b) for HF MBR [32].

stress for the planes that were measured experimentally and simulated is presented in Tab. 3.

Table 3. Overall average shear stress for the three different sparging conditions for experimental data and CFD simulations for HF MBR [32].

Air flow rate	Experimental	CFD	Error
$[m^3/h]$	[Pa]	[Pa]	[%]
5	0.25	0.24	4.65
10	0.34	0.35	0.43
15	0.49	0.45	7.65

Table 3 indicates that the error is less than 8% in term of shear stress, which shows that the average shear stress of the CFD simulations is similar to the experimental condition. This proves that the CFD model is reliable, at least in terms of average shear stress. However, as discussed earlier, the

shear profile over the membrane surface is different.

As mentioned previously, experimental measurements on shear stress were not performed for the HS MBR (Section 2.2.3). However, experimental velocity measurements were performed and a proper validation in terms of velocity profile was made [29] with error up to 11%. Therefore, it is possible to infer that the CFD model built for the HF MBR is accurate in terms of the shear stress. The results of two sheets are shown in Fig. 9.

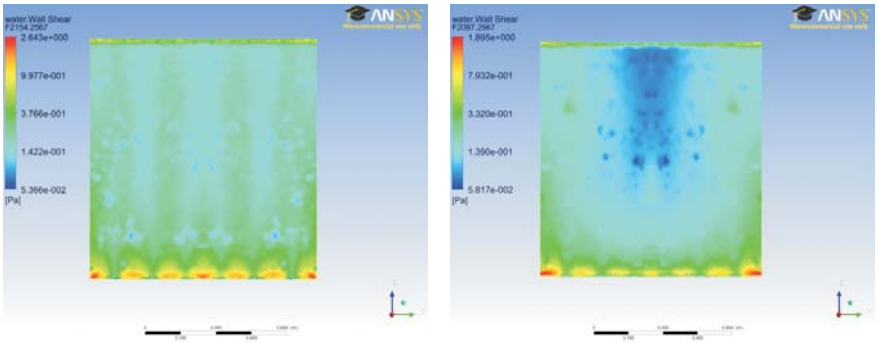

a) b)

Figure 9. Shear stress profiles (in log scale) for a HS: a) directly above the air diffusers, b) in between two air diffusers for an air flow rate of 37 m^3/h.

The overall average of shear stress for the planes is presented in Tab. 4.

Table 4. Overall average shear stress for the three different sparging conditions for the CFD simulations for HS MBR.

Air flow rate	CFD
$[m^3/h]$	[Pa]
37	0.21
55	0.31
74	0.38

Based on the CFD results (Tabs. 3 and 4) and the relationship of shear stress for bubble columns (Section 2.3), a correction factor (m) is introduced into Eq. (16) to account for the membrane placed inside the bioreactor. The

new relationship for MBR is

$$\tau = m\left(\mu\frac{E_A}{V}\right)^{0.5}. \tag{19}$$

The correction factor, m was found using SPSS v15 (Statistical Package for the Social Sciences, IBM Corporation) [33] and a value of 0.718 ± 0.021 was determined with 95% confidence interval, with the correlation coefficient (R^2) equal to 0.928. This correction factor implies that the relationship for bubble columns is overestimated by 28% if is used for MBR systems (Fig. 10). The reason for this is that the membranes placed inside the bioreactor decrease the shear stress induced by the bubbles. Figure 10 shows the comparison of the average shear stress for the theoretical expression Eq. (16), the experimental data, CFD simulation and the new expression Eq. (19) which includes the correction factor.

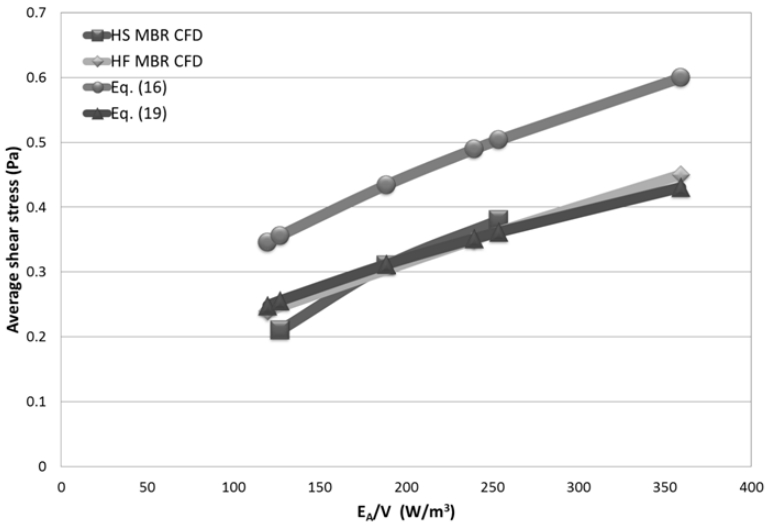

Figure 10. Average shear stress vs. E_A/V for HS MBR, HF MBR, theoretical expression for bubble columns, Eq. (16), and empirical relationship, Eq. (19).

Figure 10 clearly shows that the relationship for bubble columns is overestimated for the MBR system. Therefore, a new relationship is made including a correction factor to account for the membranes placed inside the bioreactor. The relationship made in this contribution can be used for either HF or HS MBR which broadens its applicability. However, it is important

to highlight that this empirical relationship is only valid for a system with similar geometries working under similar operational conditions.

As experimental wall shear stress measurements (i.e. electrolyte solution) cannot be used with activated sludge due to the heterogeneity of it. It is necessary to extrapolate the results obtained from the CFD simulations of water to activated sludge. The blower power equation (7) is independent of the viscosity, and the density of sludge is just 0.2% larger than water [18]. Thus, it should not affect the results of the blower power. Therefore, Eq. (17) can be modified directly including the correction factor (m), then, the linear relationship for activated sludge becomes:

$$\tau = m\left[k\left(\frac{E_A}{V}\right)^n\right]^{\frac{1}{n+1}} . \tag{20}$$

The result for three different total suspended solids (TSS) concentrations is presented in Fig. 11.

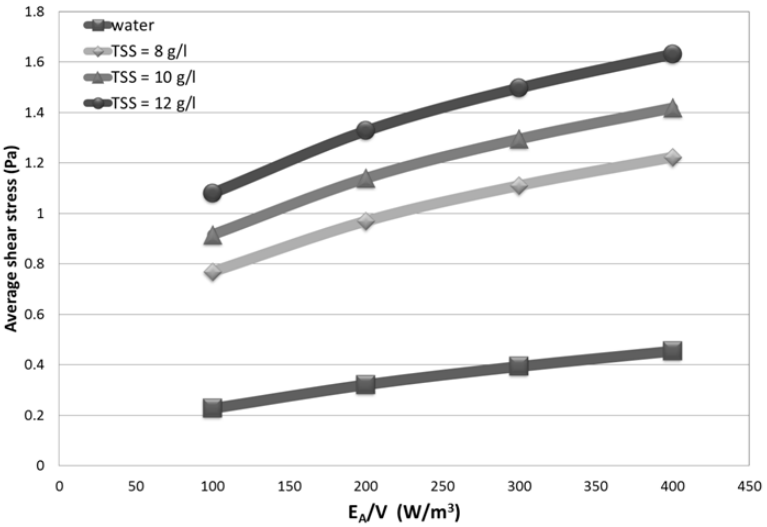

Figure 11. Average shear stress vs. E_A/V for water and three TSS concentrations (8, 10 and 12 g/l.

Figure 11, shows that including the non-Newtonian behaviour of sludge, the average wall shear stress is roughly 3.5 times larger than for water. Based on that, it is possible to affirm that including the viscosity in shear stress analysis is a must in the study of MBR systems, for experimental measurements and CFD simulations.

4 Conclusions

Two CFD models were developed: HF and HS MBR. For the HF system, experimental measurements (i.e. shear stress) were made and the results were compared with the CFD simulations. An error less than 8% was found between the measurements and CFD simulations in terms of average wall shear stress. For the HS system, experimental measurements (i.e. velocity) were completed and the results were compared with the CFD simulations. An error less than 11% was found between the measurements and CFD simulations in terms of velocity profiles. This proved that the CFD model was reliable. It can be concluded that:

- Blower power consumption depends on the air flow rate. Therefore, the HS MBR has a larger energy consumption, due to the high air flow rates applied to the systems, compared to HF MBR. Considering the blower power per unit of permeate (the two MBR systems operates at the same permeate flux), the HS requires less energy per cubic meter of permeate.
- The shear stress relationship (Eq. (16)) for bubble columns is overestimated for MBR systems by 28% compared to the CFD results. The reason for this is that the relationship for bubble columns does not take into account the membranes placed inside the reactor, affecting the bubbles movements.
- A new relationship was made (Eq. (19)) which includes a correction factor to account for the membranes. This relationship can be used for both systems; HF and HS MBRS. However, as it is an empirical relationship, care must be taken if used in systems with different geometries and different operational conditions.
- An extrapolation to determine the average shear stress in MBR systems was made to account for the non-Newtonian behaviour of activated sludge (Eq. (20)). The viscosity was found to have a strong impact on the average shear stress (up to 3.5 times larger than water); therefore, it should be considered for design purposes and future CFD models.

Acknowledgments The surface shear forces were obtained from the UBC Filtration Technology Group (University of British Columbia, Vancouver, Canada).

APPENDIX A

The geometrical description of the variables presented in Tab. 1 is presented in Fig. A1.

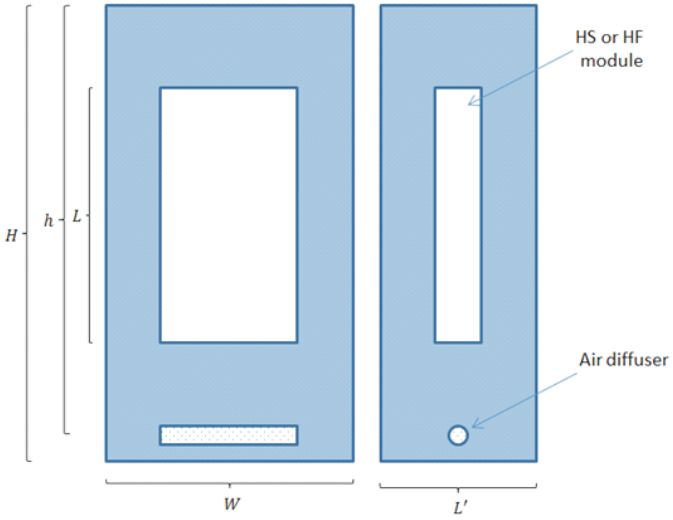

Figure A1. Schematic of a tank with a membrane module.

The hollow fiber (HF) and the hollow sheet (HS) of the submerged membrane bioreactors (MBR) are shown in Fig. A2.

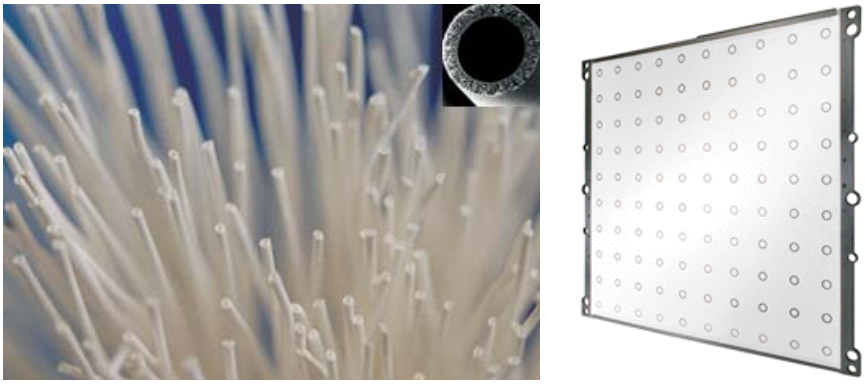

(a) (b)

Figure A2. The submerged membrane bioreactors: a) HF and b) HS MBRs.

Received 27 December 2011

References

[1] Judd S.: *The MBR Book* Elsevier, 2006.

[2] Mosdorf R., Wyszkowski T., Dąbrowski K.: *Multifractal properties of large bubble paths in a single bubble column.* Archives of Thermodynamics **32**(2011), 1, 3–20

[3] Buwa V.V., Ranade V.V.: *Dynamics of gas-liquid flow in a rectangular bubble column: experiments and single/multi-group CFD simulations.* Chem. Eng. Sci. **5**(2011) 4715–4736.

[4] Svendsen H.F., Jakobsen H.A., Torvik R.: *Local flow structures in internal loop and bubble column reactors.* Chem. Eng. Sci. **47**(2009) 3297–3304.

[5] Judd S.J.: *A review of fouling of membrane bioreactors in sewage treatment.* Water Sci. Technol. **49**(2004), 2, 229–235.

[6] Liao B.Q., Bagley D.M., Kraemer H.E., Leppard G.G., Liss S.N.: *A review of biofouling and its control in membrane separation bioreactors.* Water Environ. Res. **76**(2004) 5, 425–436.

[7] Bellara S.: *Gas sparging to enhance permeate flux in ultrafiltration using hollow fibre membranes.* J. Membr. Sci. **121**(1996), 2, 175–184.

[8] Berube P.R., Afonso G., Taghipour F., Chan C.C.V.: *Quantifying the shear at the surface of submerged hollow fiber membranes.* J. Membr. Sci. **279**(2006), 1-2, 495–505.

[9] Cui Z.F., Wright K.I.T.: *Flux enhancements with gas sparging in downwards crossflow ultrafiltration: Performance and mechanism.* J. Membr. Sci. **117**(1996), 1-2, 109–116.

[10] Cui Z.F., Chang S., Fane A.G.: *The use of gas bubbling to enhance membrane processes.* J. Membr. Sci. **221**(2003) 1-2 109–116.

[11] Katsoufidou K., Yiantsios S.G., Karabelas A.J.: *A study of ultrafiltration membrane fouling by humic acids and flux recovery by backwashing: Experiments and modeling.* J. Membr. Sci. **266**(2005), 1-2, 40–50.

[12] Yeo A.P.S., Law A.W.K., Fane A.G.: *Factors affecting the performance of a submerged hollow fiber bundle.* J. Membr. Sci. **280**(2006), 1-2, 969–982.

[13] Yeo A.P.S., Law A.W.K., Fane A.G.: *The relationship between performance of submerged hollow fibers and bubble-induced phenomena examined by particle image velocimetry.* J. Membr. Sci. **304**(2007), 1-2, 125–137.

[14] Ducom G., Puech F.P., Cabassud C.: *Air sparging with flat sheet nanofiltration: A link between wall shear stresses and flux enhancement.* Desalination **145**(2002), 1-3, 97–102.

[15] Ducom G., Puech F.P., Cabassud C.: *Gas/liquid two-phase flow in a flat sheet filtration module: Measurement of local wall shear stresses.* Can. J. Chem. Eng. **81**(2003), 3-4, 771–775.

[16] Judd S.: *Theoretical and experimental representation of a submerged membrane bio-reactor system*. Membr. Technol. **135**(2001), no. 135, 4–9.

[17] Verrecht B., Judd S., Guglielmi G., Brepols C., Mulder J.W.: *An aeration energy model for an immersed membrane bioreactor*. Water Res. **42**(2008), 19, 4761–4770.

[18] Tchobanoglous G., Burton F.L., Stensel H.D.: *Wastewater Engineering: Treatment and Reuse*. McGraw-Hill, Boston 2003.

[19] Yang F., Bick A., Shandalov S., Brenner A., Oron G.: *Yield stress and rheological characteristics of activated sludge in an airlift membrane bioreactor*. J. Membr. Sci. **334**(2009), 83-90.

[20] Laera G., Giordano C., Pollice A., Saturno D., Mininni G.: *Membrane bioreactor sludge rheology at different solid retention times*. Water Res. **41**(2007), no. 18, 4197–4203.

[21] Pollice A., Giordano C., Laera G., Saturno D., Mininni G.: *Rheology of sludge in a complete retention membrane bioreactor*. Environ. Tech. **27**(2006), no. 7, 723–732.

[22] Rosenberger R., Kubin K., Kraume M.: *Rheology of Activated Sludge in Membrane Bioreactors. Engineering in Life Sciences* **2**(2002), no. 9, 269–275.

[23] Sanchez J., Perez A., Rodriguez Porcel E.M., Casas Lopez J.L., Fernandez Sevilla J.M., Chisti Y.: *Shear rate in stirred tank and bubble column bioreactors*. Chem. Eng. J. **124** (2006), 1.

[24] Legrand J., Dumont E., Comiti J., Fayolle F.: *Diffusion coefficients of ferricyanide ions in polymeric solutions — comparison of different experimental methods*. Electrochim. Acta **45**(2000), 11, 1791–1803.

[25] Dumont E., Fayolle F., Legrand J.: *Flow regimes and wall shear rates determination within a scraped surface heat exchanger*. J. Food Eng. **45**(2000), 4, 195–207.

[26] Dumont E., Fayolle F., Sobolik V., Legrand J.: *Wall shear rate in the Taylor-Couette-Poiseuille flow at low axial Reynolds number*. Int. J. Heat Mass Transfer **45**(2002), 3, 679–689.

[27] Rosant J.M.: *Liquid-wall shear stress in stratified liquid/gas flow*. J. Appl. Electrochem. **24**(1994), 7, 612–618.

[28] Fulton B., Redwood J., Tourais M. and Bérubé P.R.: *Distribution of Surface Shear Forces and Bubble Characteristics in Full-Scale Gas Sparged Submerged Hollow Fiber Membrane Modules*, Desalination, 2011, 281, 128–141.

[29] Bentzen T.R., Ratkovich N., Rasmussen M.R., Heinen N., Hansen F.: *Energy efficient aeration in a single low pressure hollow sheet membrane filtration module*. G W F – Wasser, Abwasser **152**(2011), 104–107.

[30] Kulkarni A.V., Roy S.S., Joshi J.B.: *Pressure and flow distribution in pipe and ring spargers: Experimental measurements and CFD simulation*. Chem. Eng. J. **133**(2007) 1-3, 173–186.

[31] Taha T., Cui Z.F.: *Hydrodynamic analysis of upward slug flow in tubular membranes*. Desalination **145**(2002), 1-3, 179–182.

[32] Ratkovich N., Hunze M., Nopens I.: *Hydrodynamic study of a Hollow Fiber membrane system using experimental and numerical derived surface shear stresses.* Multiphase Science and Technology (in press).

[33] Argyrous G.: *Statistics for Research: With a Guide to SPSS*, 2nd edn, Sage, London 2005.